Acid Denaturation and Refolding of Green Fluorescent Protein†

Sawako Enoki, Kimiko Saeki, Kosuke Maki, and Kunihiro Kuwajima*

Department of Physics, School of Science, The University of Tokyo, 7-3-1 Hongo, Bunkyo-ku, Tokyo 113-0033, Japan

Received June 18, 2004; Revised Manuscript Received September 2, 2004

ABSTRACT: Green fluorescent protein from the jellyfish *Aequorea victoria* can serve as a good model protein to understand protein folding in a complex environment with molecular chaperones and other macromolecules such as those in biological cells, but little is known about the detailed mechanisms of the in vitro folding of green fluorescent protein itself. We therefore investigated the kinetic refolding of a mutant (F99S/M153T/V163A) of green fluorescent protein, which is known to mature more efficiently than the wild-type protein, from the acid-denatured state; refolding was observed by chromophore fluorescence, tryptophan fluorescence, and far-UV CD, using a stopped-flow technique. In this study, we demonstrated that the kinetics of the refolding of the mutant have at least five kinetic phases and involve nonspecific collapse within the dead time of a stopped-flow apparatus and the subsequent formation of an on-pathway intermediate with the characteristics of the molten globule state. We also demonstrated that the slowest phase and a major portion of the second slowest phase were rate-limited by slow prolyl isomerization in the intermediate state, and this rate limitation accounts for a major portion of the observed kinetics in the folding of green fluorescent protein.

Green fluorescent protein (GFP)[1] from the jellyfish *Aequorea victoria* is a soluble globular protein consisting of 238 residues. It has a chromophore that emits green fluorescence with a maximum intensity at 508 nm and is surrounded by an 11-stranded β-barrel (*1*, *2*) (Figure 1). GFP forms the chromophore by the autocatalytic cyclization of a polypeptide backbone of Ser65, Tyr66, and Gly67 without the use of any substrate (*3*−*5*). In the native form, the chromophore is shielded from bulk water attack by the surrounding β-sheets and capping α-helices, and GFP has an extensive hydrogen bond network around the chromophore. When GFP is denatured, the chromophore undergoes attacks by water molecules, and its fluorescence is quenched. Therefore, GFP emits fluorescence only when it has the correct tertiary structure of the native form. With regard to its usefulness, the green fluorescence of GFP is commonly employed as a marker in a wide variety of studies of gene expression and protein localization.

Protein folding in biological cells is not yet well understood. However, GFP promises to be advantageous for the in vivo study of protein folding, which occurs in spaces that are crowded with numerous molecules, and hence is a process known to be mediated by molecular chaperones. Because of the green fluorescence specific to the native structure of GFP, fluorescence-detected GFP folding can be studied in a complex environment. Recently, a large number of studies using GFP as an indicator of the formation of the native structure have been reported: for example, the mechanism of the GroEL−GroES-mediated protein folding reaction (*6*−*9*).

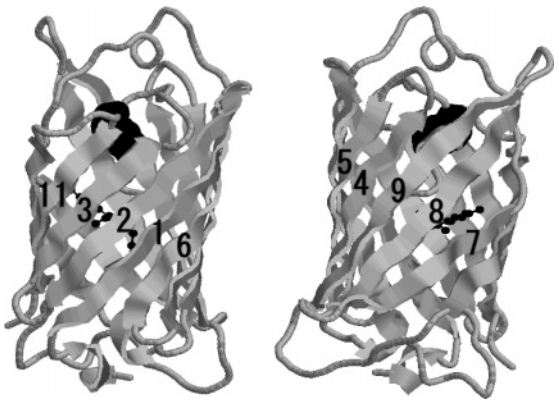

FIGURE 1: Schematic representations for the backbone structure of a GFP mutant, Cycle3 (PDB code: 1b9c), viewed from two opposite directions, drawn using RasMol. The chromophore is shown as a ball-and-stick model. The tryptophan residue is shown as a space-filling union-of-spheres model. The number is labeled for each β-strand from the N to the C terminus.

Despite the potentially useful characteristics of GFP, rather little is known about the detailed mechanisms of the folding of GFP itself in vitro. Recent studies have included those of the folding and unfolding kinetics of GFP, as monitored by chromophore fluorescence (*10*−*13*), and analysis of the structural dynamics of GFP, as monitored by NMR (*14*) and fluorescence correlation spectroscopy (*15*). In addition, pressure-induced unfolding and refolding have been monitored by static and kinetic FTIR, UV/vis, and fluorescence spectroscopy (*16*). However, to date, there has been no report on rapid folding kinetics starting from GFP in an extensively

† This work was supported by Grants-in-Aid for Scientific Research on Priority Areas (No. 15076201) from the Ministry of Education, Culture, Science, and Technology of Japan.

* Corresponding author. E-mail: kuwajima@phys.s.u-tokyo.ac.jp. Phone: (+81)-3-5841-4128. Fax: (+81)-3-5841-4512.

[1] Abbreviations: CD, circular dichroism; CyPA, cyclophilin A; DTT, dithiothreitol; EDTA, ethylenediamine-*N*,*N*,*N*′,*N*′-tetraacetic acid; FTIR, Fourier transform infrared; GdnHCl, guanidine hydrochloride; GFP, green fluorescent protein; NMR, nuclear magnetic resonance; PPIase, peptidyl−prolyl isomerase.

10.1021/bi048733+ CCC: $27.50
Published on Web 10/14/2004

unfolded state; neither has the detailed mechanism of GFP folding been described in the literature.

Here, we have investigated GFP in terms of acid denaturation and the kinetics of folding and unfolding using chromophore fluorescence, tryptophan fluorescence, and far-UV circular dichroism (CD); here, we employed a stopped-flow apparatus to investigate the rapid folding reactions starting with GFP in the denatured state. We used a mutant of GFP, Cycle3 (F99S/M153T/V163A), as the protein sample; this mutant, obtained by DNA shuffling techniques, is known to mature more efficiently in vivo than wild-type GFP (*17*). In our previous study, we discovered that the denaturation of Cycle3 is much more reversible than is that of wild-type GFP, and hence this mutant is more useful for in vitro folding studies (*10*). Furthermore, the structure of Cycle3 has been described by X-ray crystallography, and the three-dimensional structure of this mutant was found to be essentially the same as that of wild-type GFP, including the structure around the chromophore (*11*). The fluorescence spectrum of this mutant is thus the same as that of wild-type GFP. The refolding and unfolding kinetics of Cycle3 are also known to be very similar to those of wild-type GFP (*10*, *11*).

Here, we demonstrated that the kinetic folding reaction of Cycle3 undergoes at least five kinetic phases and involves nonspecific collapse within the dead time of a stopped-flow apparatus and the subsequent formation of an on-pathway intermediate that has the characteristics of the molten globule state (*18*). We also show that the slowest phase and a major portion of the second slowest phase are rate-limited by slow prolyl isomerization in the intermediate state, and this rate limitation accounts for a major portion of the observed kinetics in GFP folding.

MATERIALS AND METHODS

Protein Expression and Purification. Cycle3 was overexpressed in *Escherichia coli* and was purified from the soluble extract of *E. coli* cells by a known procedure (*10*).

Other Chemicals and Enzymes. All chemicals were of guaranteed reagent grade. Human recombinant cyclophilin A (CyPA) was purchased from Sigma (St. Louis, MO).

Methods. All equilibrium spectral measurements and kinetic refolding and unfolding measurements of Cycle3 were carried out at 25.0 °C. Protein concentration was determined by UV absorption using a molar absorption coefficient of ϵ (280 nm) = 2.06×10^4 M^{-1} cm^{-1} of Cycle3.

(1) CD and Fluorescence Spectral Measurement. Fluorescence spectral measurements were carried out in a Jasco FP-777 spectrofluorometer. The path length of optical cuvettes was 10.0 mm.

For measurement of the chromophore fluorescence spectra of Cycle3, the protein solution was excited at 395 nm, and the spectral bandwidth was set at 1.5 nm for both excitation and emission. The sample solutions were prepared in 50 mM Tris-HCl and 1 mM DTT at pH 7.5 at two different salt concentrations, 0 and 0.10 M NaCl (for the native states), and in 1 mM DTT at pH 2.0 at 0 and 0.10 M NaCl (for the acid-denatured states). The protein concentration was 0.03 mg/mL.

The tryptophan fluorescence spectra were measured as follows. The protein solution was excited at 295 nm, and the spectral bandwidth was set at 3.0 nm for both excitation and emission. The buffer solutions used for the sample preparations were the same as those described above for the chromophore fluorescence measurements. The NaCl concentrations were 0.10 M for the native state and 0 M for the denatured state. The protein concentration was 0.08 mg/mL.

CD spectral measurements were carried out in a Jasco J-720 spectropolarimeter. The path length of the optical cuvettes was 1.0 mm, and the spectral bandwidth was 1.0 nm. The samples used for CD measurements were prepared in the same buffer solution as that used for the fluorescence measurements, except for the pH of the acid-denatured state (pH 1.5). The protein concentration was 0.17 mg/mL. The far-UV CD spectrum of the protein in the guanidine hydrochloride (GdnHCl) unfolded state was measured in 20 mM potassium phosphate buffer, pH 7.0, containing 1 mM EDTA, 1 mM DTT, and 6 M GdnHCl, at 0.5 mg/mL Cycle3 (*10*).

The apparent transition curves for unfolding and refolding were measured by the fluorescence intensity at 508 nm at 0 and 0.10 M NaCl. The protein stock solutions at 0 M NaCl were prepared in 18 mM Tris-HCl plus 1 mM DTT at pH 7.5 for the unfolding reactions and in 1 mM DTT at pH 2.0 for the refolding reactions. The stock solutions at 0.10 M NaCl were prepared in 18 mM Tris-HCl and 0.10 M NaCl plus 1 mM DTT at pH 7.5 for the unfolding reactions and in 0.10 M NaCl plus 1 mM DTT at pH 2.0 for the refolding reactions. After the samples were incubated for 30 min at room temperature, the stock solutions were diluted into either an unfolding or a refolding buffer for measurement. The final protein concentration was 0.03 mg/mL, and the final solutions at 0 M NaCl contained 18 mM Tris-HCl (above pH 7.0), BisTris (from pH 6.0 to pH 7.0), or CH_3COONa (from pH 3.5 to pH 5.5) as a buffer salt and 1 mM DTT, and the solutions at 0.10 M NaCl contained 50 mM Tris-HCl, BisTris, or CH_3COONa as a buffer salt and 0.10 M NaCl and 1 mM DTT.

The apparent transition curves for the unfolding reactions were also measured by CD at 225 nm at 0 and 0.10 M NaCl. The sample preparations and the protein concentrations were the same as those shown above for the fluorescence measurements.

(2) Estimation of Secondary Structure Fractions. We estimated the fractions of the secondary structures in the native and acid-denatured states of Cycle3 based on the far-UV CD spectra of the protein. The observed ellipticity, θ_{obs}, at any fixed wavelength can be expressed by a linear combination of the ellipticity values, θ_α, θ_β, and θ_c, of the three reference spectra for the α-helix, β-structure, and coil, respectively, as

$$\theta_{obs} = f_\alpha\theta_\alpha + f_\beta\theta_\beta + f_c\theta_c \quad (1)$$

where f_α, f_β, and f_c are α-helix, β-structure, and coil fractions, respectively. The values of f_α, f_β, and f_c were estimated by linear least squares with a constraint of $f_\alpha + f_\beta + f_c = 1$. We also analyzed the spectra with four reference spectra for the α-helix, β-sheet, β-turn, and coil in the same manner. The reference spectra of Greenfield and Fasman (*19*) and those of Brahms and Brahms (*20*) were used.

(3) Kinetic Fluorescence Measurements. (a) Chromophore Fluorescence. We performed the kinetic refolding measure-

ments using a SX.18MV stopped-flow fluorescence apparatus (Applied Photophysics). The dead time of the apparatus was 5 ms. The excitation wavelength was 395 nm, and the emission of fluorescence was detected using a 460 nm cutoff filter (SC-46, Fuji Photo Film Co.).

For the data for which the final pH was 7.5 (Figure 4a and Table 2), the refolding reactions were started by mixing denatured Cycle3 (1 mM DTT at pH 2.0) with a refolding buffer at a ratio of 1:10.4. The final solution contained 0.075 mg/mL Cycle3 in 50 mM Tris-HCl, 0.10 M NaCl, and 1 mM DTT at pH 7.5.

With regard to the data at various final pH values (Figure 5), the final concentration of Cycle3 was 0.02 mg/mL. The final solution contained 0.10 M NaCl, 1 mM DTT, and 50 mM Tris-HCl (from pH 7.5 to pH 8.5), BisTris (from pH 6.0 to pH 7.0), or CH3COONa (below pH 5.5).

We also performed kinetic unfolding measurements in the Applied Photophysics SX.18MV stopped-flow fluorescence apparatus when the final pH was ≤3.5 at both 0 and 0.10 M NaCl, and in addition, a Jasco FP-777 spectrofluorometer was used under conditions of manual mixing when the final pH was ≥3.9 at 0.10 M NaCl. The protein concentration was 0.01−0.03 mg/mL. The unfolding reactions were started by mixing the native Cycle3 (10 mM Tris-HCl, the indicated NaCl concentration, and 1 mM DTT at pH 7.5) with the unfolding buffer at a ratio of 1:10.4 for the stopped-flow measurements and 1:9 for the manual mixing measurements. The final solutions obtained at pH ≤3.5 contained the indicated NaCl concentration plus 1 mM DTT, and those at pH ≥3.9 contained 0.10 M NaCl, 45 mM HCOONa, and 1 mM DTT.

Native to denatured to native (NDN) double-jump experiments were performed in the Applied Photophysics SX.18MV stopped-flow apparatus in a double-mixing mode. Native Cycle3 at pH 7.5 in 10 mM Tris-HCl and 1 mM DTT was first mixed with an unfolding buffer at a ratio of 1:1, giving a denatured protein solution that contained 1 mM DTT at pH 2.0. After an aging period (t_a), the second mixing with a refolding buffer at a ratio of 1:1 prevented the protein from further denaturation and refolded the already denatured protein molecules. The final solution contained 0.01 mg/mL Cycle3 in 50 mM Tris-HCl, 0.10 M NaCl, and 1 mM DTT at pH 7.5.

We also performed kinetic refolding measurements in the presence and absence of CyPA in a Jasco FP-777 spectrofluorometer by manual mixing. The refolding reactions were started by mixing denatured Cycle3 (1 mM DTT at pH 2.0) with a refolding buffer that contained CyPA, at a volume ratio of 1:1. The final solution contained 0.02 mg/mL (0.75 μM) Cycle3 and 0.038 mg/mL (2.1 μM) CyPA in 20 mM Tris-HCl and 1 mM DTT at pH 7.5.

(b) Tryptophan Fluorescence. The kinetic refolding and unfolding reactions monitored by tryptophan fluorescence were also measured in the Applied Photophysics SX.18MV stopped-flow apparatus. The excitation wavelength was 295 nm, and the emission of fluorescence was detected using a band-pass filter (U-350; Hoya Co.), through which light centered at 350 nm was transmitted.

The refolding reactions were started by mixing denatured Cycle3 in 1 mM DTT at pH 2.0 with a refolding buffer at a ratio of 1:1. The final solution contained 0.04 mg/mL Cycle3 in 50 mM Tris-HCl, 0.10 M NaCl, and 1 mM DTT at pH 7.5.

The unfolding reactions were started by mixing the native Cycle3 in 0.6 mM Tris-HCl and 1 mM DTT at pH 7.0 with an unfolding buffer at a ratio of 1:1. The final solution contained 0.04 mg/mL Cycle3 in 1 mM DTT at pH 2.

(4) Kinetic CD Measurements. The kinetic CD measurements were performed using a stopped-flow apparatus (specially constructed by Unisoku, Inc., Osaka, Japan) attached to the Jasco J-720 spectropolarimeter. The wavelength for the measurement was set at 225 nm. The dead time of the apparatus was 25 ms. The refolding reactions were started by mixing denatured Cycle3 in 1 mM DTT at pH 2.0 with a refolding buffer at a ratio of 10.6:1. The final concentration of Cycle3 was 0.074 mg/mL. The final solution at 0.10 M NaCl also contained 50 mM Tris-HCl, 0.10 M NaCl, and 1 mM DTT, and the final solution at 0 M NaCl also contained 20 mM Tris-HCl and 1mM DTT, whereby the final pH was pH 7.5.

(5) Kinetic Analysis. The kinetic data were fitted by nonlinear least squares using the equation:

$$A(t) = A(\infty) - \sum \Delta A_i e^{-k_i t} \quad (2)$$

where $A(t)$ and $A(\infty)$ are the fluorescence intensities (or the mean residue ellipticities) at time t and the infinite time, respectively; in addition, ΔA_i and k_i are the amplitude and the apparent rate constant of the ith phase, respectively.

RESULTS

Fluorescence and CD Spectra of Native and Acid-Denatured Cycle3. Native and acid-denatured Cycle3 have been characterized by the fluorescence emission spectra of the green fluorescent (*p*-hydroxybenzylideneimidazolidone) chromophore and a tryptophan residue and by the far-UV CD spectra obtained for the protein.

Figure 2a shows the chromophore fluorescence spectra excited at 395 nm. We measured the spectra at two different salt concentrations (0 and 0.10 M NaCl). The fluorescence spectra of native Cycle3 under these conditions are essentially identical and revealed a single peak at 508 nm, with a small shoulder on the side with the longer wavelength. The acid denaturation process was accompanied by the loss of fluorescence, and no emission was observed in the denatured state under both conditions.

Figure 2b shows the tryptophan fluorescence spectra, excited at 295 nm, in the native state at pH 7.5 and 0.10 M NaCl and in the acid-denatured state at pH 2.0 and 0 M NaCl. When Cycle3 was acid-denatured, the peak of the spectrum of Cycle3 shifted to a longer wavelength, i.e., from 330 to 347 nm, which may have been the result of the exposure of a tryptophan residue from the protein's interior to solvent water.

Figure 2c shows the far-UV CD spectra of native and acid-denatured Cycle3 at 0 and 0.10 M NaCl. The native CD spectrum showed a broad negative band near 217 nm, suggesting a significant spectral contribution from the β-structure. The CD spectra of the acid-denatured state at 0 and 0.10 M NaCl both revealed a disruption of the native secondary structure and had the characteristics of an unfolded protein. However, the protein at 0 M NaCl was more unfolded than the protein at 0.10 M NaCl. This finding was

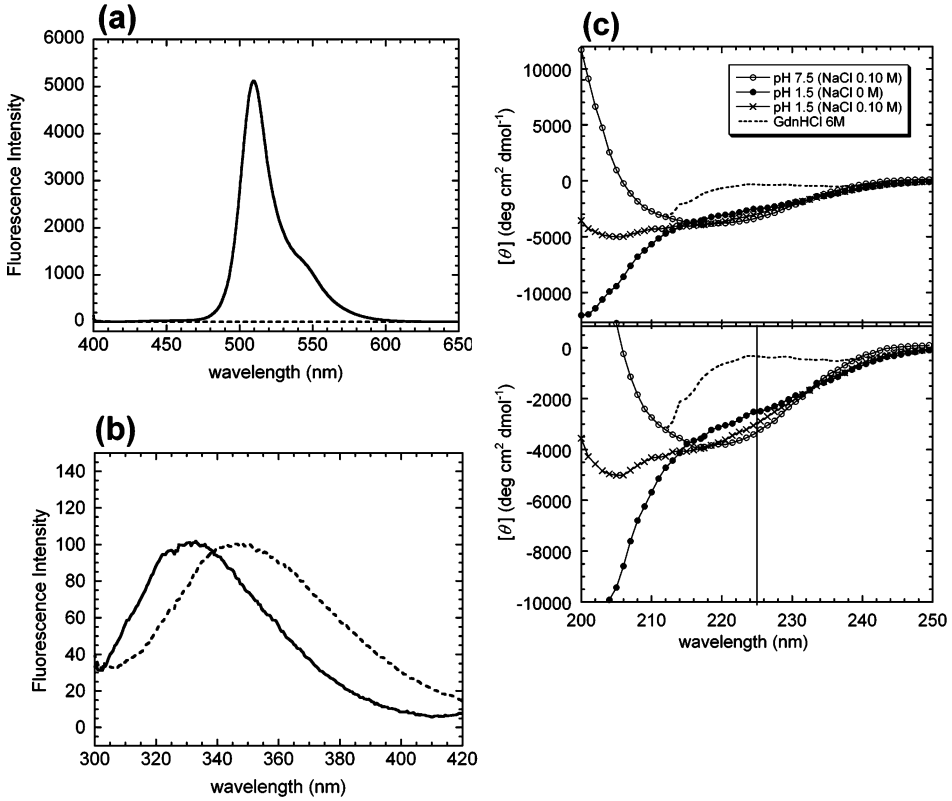

FIGURE 2: (a) Chromophore fluorescence spectra of Cycle3 excited at 395 nm. Solid and dotted lines show the spectra in the native state (0.10 M NaCl and 50 mM Tris-HCl, at pH 7.5) and the denatured state (0.10 M NaCl, at pH 2.0), respectively. (b) Tryptophan fluorescence spectra of Cycle3 excited at 295 nm. Solid and dotted lines show the spectra in the native state (0.10 M NaCl and 50 mM Tris-HCl, at pH 7.5) and the denatured state (0 M NaCl, at pH 2.0), respectively. (c) Far-UV CD spectra of Cycle3. Open circles (○), crosses (×), and closed circles (●) show the spectra in the native state (0.10 M NaCl and 50 mM Tris-HCl, at pH 7.5), the denatured state at 0.10 M NaCl and pH 1.5, and the denatured state at 0 M NaCl and pH 1.5. A broken line represents the spectrum of Cycle3 in 6 M GdnHCl (*10*). The magnified spectra are shown in the lower panel. A vertical solid line in the lower panel shows the wavelength at 225 nm. Measurements of the unfolding transition curve and kinetic refolding curve were carried out at 225 nm.

Table 1: Secondary Structure Contents of Cycle3 in the Native State, Denatured State at 0.10 M NaCl, and Denatured State at 0 M NaCl, As Estimated from the CD Spectral Data of Figure 2c

		α-helix	β-sheet	β-turn	coil
Greenfield	pH 7.5 (0.10 M NaCl)	4	75		21
and	pH 1.5 (0.10 M NaCl)	7	43		49
Fasman	pH 1.5 (0 M NaCl)	9	24		67
Brahms	pH 7.5 (0.10 M NaCl)	−3	65	9	29
and	pH 1.5 (0.10 M NaCl)	6	39	10	45
Brahms	pH 1.5 (0 M NaCl)	9	27	8	56

most likely due to the binding of chloride ions to the acid-denatured protein, which would minimize intramolecular charge repulsion and stabilize the secondary structure that is retained in the denatured protein.

We calculated the fractions of the secondary structures in native and acid-denatured Cycle3 from the spectra of Figure 2c by various methods; this was done in order to estimate the conformation of proteins from the CD data. Among the different methods tested, those employing the reference spectra of Greenfield and Fasman (*19*) and the reference spectra of Brahms and Brahms (*20*) gave good fits with the present data (Table 1). The results revealed that the β-structure content of acid-denatured Cycle3 was lower and the irregular structure content was higher than those of native Cycle3. Furthermore, this trend was more remarkable at 0 M NaCl. Although the decrease in the salt concentration resulted in greater disruption of the structure in the acid-denatured state, the protein was not fully unfolded. Thus, a significant amount of the secondary structure was observed even at 0 M NaCl, as compared with the structure in the fully unfolded state at a high concentration of a strong denaturant such as GdnHCl or urea; the CD spectrum of Cycle3 in 6 M GdnHCl is included for comparison in Figure 2c.

Unfolding Transition Curves. The unfolding and refolding transitions of Cycle3 were induced by acidification of the native protein solution and neutralization of the acid-denatured protein solution, respectively, and these reactions were followed by the chromophore fluorescence at 508 nm. We measured the transition curves at two salt concentrations, 0 and 0.10 M NaCl, and the results are shown in Figure 3a. The data in Figure 3a are those measured after time-dependent fluorescence changes were saturated. Because the unfolding and the refolding transition curves were not coincident with each other, the unfolding transition was not fully reversible (Figure 3a) (*21*, *22*); however, greater reversibility was observed at 0 M NaCl than at 0.10 M NaCl. Neutralization of the acid-denatured protein restored 90% of the native fluorescence when Cycle3 was refolded at pH 7 from the denatured state at pH 2.0 and at 0 M NaCl.

The unfolding transition curves were also measured by the far-UV CD at 225 nm at 0 and 0.10 M NaCl (Figure 3b). The apparent midpoint of the transition measured by CD at 225 nm was at a lower pH, especially at 0.10 M NaCl,

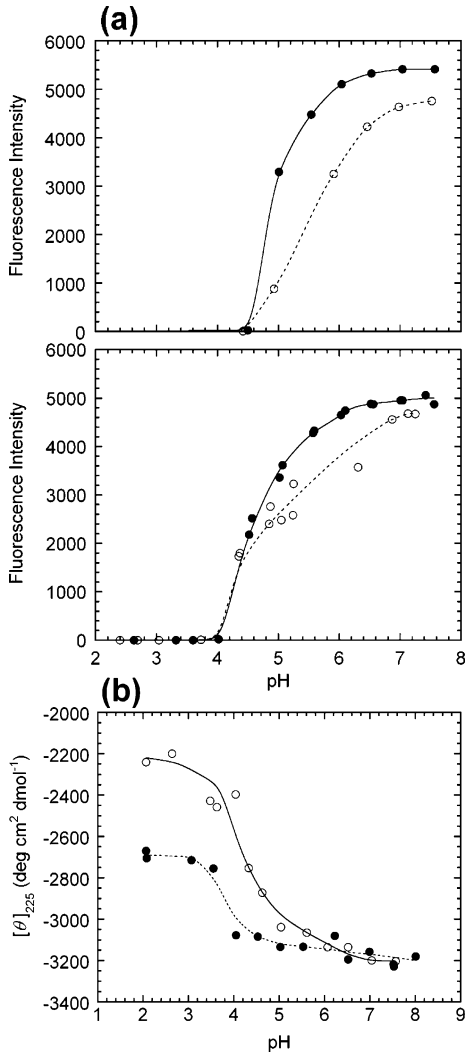

FIGURE 3: (a) Unfolding and refolding transition curves of Cycle3 measured by fluorescence at 508 nm and excited at 395 nm. The translation curves were measured at 0.10 M NaCl (upper panel) and at 0 M NaCl (lower panel). Closed circles (●) and a solid line show the unfolding transition curves, and the open circles (○) and a dotted line show the refolding curves. (b) Unfolding transition curves measured by the far-UV CD at 225 nm. A solid line with open circles (○) and a dotted line with closed circles (●) show the transition curves measured at 0 M NaCl and 0.10 M NaCl, respectively.

than the apparent midpoint measured by the fluorescence at 508 nm.

The percent reversibility of the unfolding transition depended not only on the refolding conditions but also on the conditions used for unfolding the protein, such as incubation time and the salt (NaCl) concentration under the acid-denaturing condition. As the incubation time under the denaturing condition became longer, the percent reversibility decreased. The reversibility, as measured by the chromophore fluorescence of Cycle3, from the acid-denatured state at 0 M NaCl was more pronounced than the reversibility from the same state at 0.10 M NaCl, even when the identical refolding conditions were used (data not shown).

The far-UV CD spectrum of Cycle3 refolded from the acid-denatured state at 0 M NaCl was the same as that of native Cycle3 (data not shown). However, the far-UV CD spectrum of the protein refolded from the acid-denatured state at 0.10 M NaCl was more intense than that of the original native protein spectrum, indicating the presence of the non-native conformation in the refolded protein. This result was probably caused by aggregation during either refolding or incubation under the denaturing condition. It appears that Cycle3 tends to aggregate at pH 2, especially at a high salt concentration.

Kinetic Measurements. We investigated the refolding and unfolding kinetics by measuring chromophore fluorescence, tryptophan fluorescence, and the far-UV CD of Cycle3.

(1) Refolding. Figure 4a shows a typical kinetic refolding curve measured by the chromophore fluorescence excited at 395 nm. The refolding of the protein was started by a stopped-flow pH (and NaCl concentration) jump from pH 2.0 and 0 M NaCl to pH 7.5 and 0.10 M NaCl, and the fluorescence emission above 460 nm was monitored. The refolding curve of Cycle3 was fitted with four exponentials above pH 6 and with three exponentials below pH 6. Essentially the same refolding kinetics were observed in the absence of NaCl (Table 2), such that the refolding kinetics measured by the chromophore fluorescence did not appear to depend on the presence or absence of NaCl. It was of note that the sign of the amplitude of the most rapid observed phase above pH 6 was the opposite of those of the subsequent phases (see also Figure 5). Because chromophore fluorescence monitors the formation of the native structure, the most rapid observed phase with the opposite amplitude may represent a lag phase resulting from the accumulation of an on-pathway folding intermediate. The measured refolding kinetics appear not to have been affected by aggregation, as the refolding kinetics were essentially the same at various Cycle3 concentrations ranging from 0.005 to 0.075 mg/mL.

Panels a and b of Figure 5 show the apparent rate constants and the relative amplitudes, respectively, of the individual phases of the multiexponential fit of the observed kinetics, which are plotted as a function of pH. None of the apparent rate constants of any of the four phases revealed any remarkable changes when the final pH was changed from pH 8 to pH 5.5, whereas the absolute values of the amplitudes of the very fast and the fast phases were reduced when the final pH was decreased. The amplitude of the medium phase was first increased until the pH level reached 6, and then the amplitude decreased with decreases in the final pH. The amplitude of the slow phase increased when the final pH decreased.

Figure 4b shows a typical kinetic refolding curve measured by the tryptophan fluorescence intensity using the stopped-flow apparatus. The refolding of the protein was initiated by a pH (and NaCl concentration) jump from the denatured state at pH 2.0 and 0 M NaCl to the native state at pH 7.5 and 0.10 M NaCl, and the fluorescence intensity was monitored through a 350 nm band-pass filter. The fluorescence intensity rapidly increased within the dead time (5 ms) of the stopped-flow apparatus and then decreased with a four-exponential kinetics. This decrease in tryptophan fluorescence may have been caused by the quenching of fluorescence emission by nearby groups or molecules, including the *p*-hydroxybenzylideneimidazolidone chromophore as well as solvent water molecules; only a single tryptophan residue (Trp57) 11 Å apart from the chromophore in the native structure of Cycle3 is present (Figure 1). The most rapid phase of the observable (fluorescence-decreasing) kinetics has a rate constant that is apparently faster than the rate

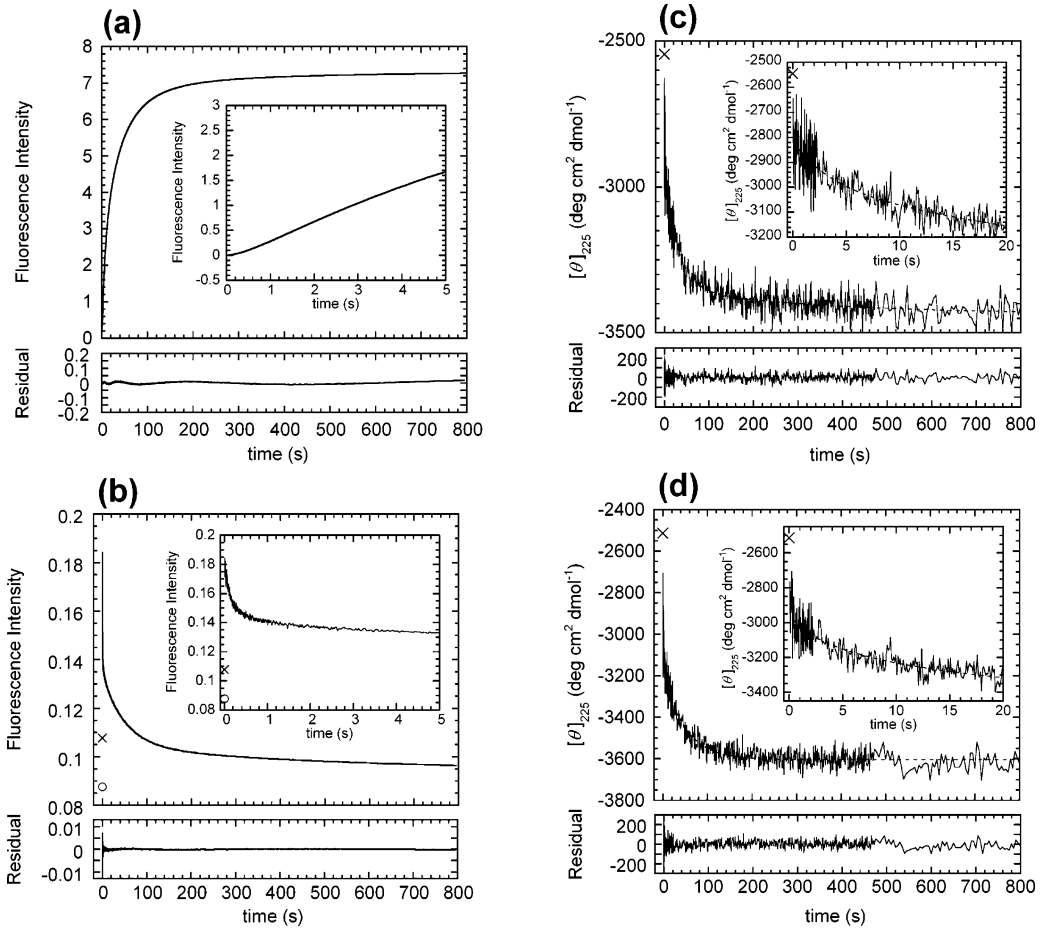

FIGURE 4: Kinetic refolding curves of Cycle3 monitored by (a) chromophore fluorescence excited at 395 nm, (b) tryptophan fluorescence excited at 295 nm, (c) CD at 225 nm at 0.10 M NaCl, and (d) CD at 225 nm at 0 M NaCl. The broken lines show the theoretical curves best fit to the experimental data, and the best-fit values of the rate constants and amplitudes are given in Table 2. The lower panel in each part shows the residual plot. The reactions were initiated by a pH/NaCl concentration jump from pH 2.0 and 0 M NaCl to pH 7.5 and 0.10 M NaCl for (a), (b), and (c). The reactions were initiated by a pH jump from pH 2.0 and 0 M NaCl to pH 7.5 and 0 M NaCl for (d). The inset of (a) shows the refolding curve within 5 s. We can see a lag phase, the rate constant of which is 2.19 s^{-1}. (b) Crosses and open circles represent the fluorescence intensities of the denatured and the native states, respectively. Here, the fluorescence intensity clearly increases rapidly within the dead time (5 ms) and then decreases. The inset of (b) shows the refolding curve within 5 s. (c, d) The cross in the each part represents the CD ellipticity of the denatured state. Each inset of (c) and (d) shows the refolding curve within 20 s.

Table 2: Rate Constants and Normalized Amplitudes of Refolding Curves of Cycle3 Measured by Chromophore Fluorescence at 0.10 and 0 M NaCl, by CD at 225 nm at 0.10 and 0 M NaCl, and by Tryptophan Fluorescence at 0.10 M NaCl and at 25.0 °C[a]

	[NaCl] (M)		rate constant k (s^{-1}) and relative amplitude A (%)				
			burst	very fast	fast	medium	slow
chromophore fluorescence	0.10	k		2.19 ± 0.04	0.154 ± 0.001	0.0270 ± 0.0001	0.00591 ± 0.00006
		A	0	−2.95 ± 0.03	34.5 ± 0.09	55.4 ± 0.1	13.1 ± 0.1
chromophore fluorescence	0	k		2.54 ± 0.09	0.205 ± 0.002	0.0346 ± 0.0006	0.01125 ± 0.00043
		A	0	−3.89 ± 0.08	38.8 ± 0.3	51.5 ± 0.7	13.7 ± 0.9
far-UV CD	0.10	k			0.311 ± 0.066	0.0317 ± 0.0050	0.00287 ± 0.00227
		A	30.1		17.9 ± 2.6	42.1 ± 2.6	9.83 ± 1.87
far-UV CD	0	k		3.67 ± 1.02	0.206 ± 0.052	0.0205 ± 0.0015	
		A	29.3	14.4 ± 1.8	17.0 ± 1.6	39.4 ± 1.8	
tryptophan fluorescence	0.10	k		7.36 ± 0.19	0.690 ± 0.045	0.0239 ± 0.001	0.00361 ± 0.00060
		A	−621	279 ± 4	102 ± 3	239 ± 9	100 ± 7
far-UV CD (fixed k)[b]	0.10	k		2.19	0.154	0.0270	0.00591
		A	29.3	4.82 ± 1.46	22.0 ± 1.6	34.0 ± 2.2	9.87 ± 1.66
far-UV CD (fixed k)[b]	0	k		2.19	0.154	0.0270	0.00591
		A	31.1	14.6 ± 1.2	13.4 ± 1.3	33.7 ± 1.8	7.31 ± 1.39

[a] The relative amplitudes for the denatured state and the refolded state were 0% and 100%, respectively. [b] The rate constants were fixed to the values of the kinetics measured by the chromophore fluorescence at 0.10 M NaCl.

constant for the lag (fastest) phase, as observed by chromophore fluorescence (see Table 2). This finding indicates that the on-pathway folding intermediate formed during the lag phase must have quite a compact structure, such that the tryptophan fluorescence was partially quenched by the chromophore.

Panels c and d of Figure 4 show typical kinetic refolding curves measured at 0.10 and 0 M NaCl, respectively, by the

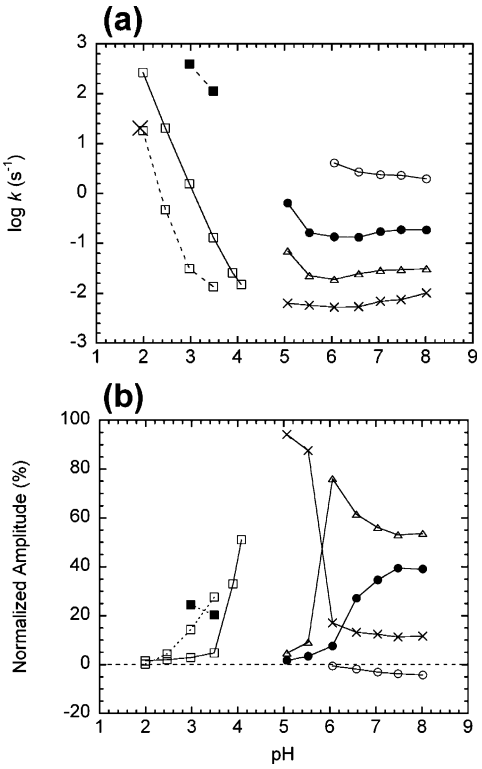

FIGURE 5: pH dependence of the apparent rate constants (a) and normalized amplitudes (b) of the refolding and unfolding kinetics of Cycle3, as measured by the chromophore fluorescence excited at 395 nm and tryptophan fluorescence excited at 295 nm. Open circles, closed circles, open triangles, and small crosses show the very fast, fast, medium, and slow phases of the refolding kinetics monitored by chromophore fluorescence, respectively. Open squares and a solid line show the unfolding kinetics from pH 7.5 and 0 M NaCl to the indicated pH and 0.10 M NaCl, as monitored by chromophore fluorescence. Open squares and a dotted line and closed squares and a dotted line show the slow and fast phases of the unfolding kinetics from pH 7.5 and 0 M NaCl to the indicated pH and 0 M NaCl, respectively, as monitored by the chromophore fluorescence. A large cross indicates the unfolding kinetics from pH 7.5 and 0 M NaCl to the indicated pH and 0 M NaCl monitored by the tryptophan fluorescence.

CD at 225 nm in the stopped-flow CD apparatus. The refolding process was initiated by a pH (and NaCl concentration) jump from pH 2.0 (0 M NaCl) to pH 7.5 (i.e., the indicated concentration of NaCl). The changes occurring within the burst phase amounted to 30%, irrespective of the NaCl concentration. The refolding curves at both 0.10 and 0 M NaCl were fitted with at least three exponentials. At 0 M NaCl, there was a rapid increase, the rate constant (3.67 $\pm$ 1.02 s^{-1}) of which was close to that of the lag phase observed by the refolding monitored by chromophore fluorescence. We were unable to analyze the refolding kinetics with more than three exponentials due to a low signal-to-noise ratio. Because reactions monitored by different probes should show the same rate constants, we also analyzed the data with the four rate constants fixed to those of the refolding monitored by chromophore fluorescence (Table 2). In this regard, the results showed excellent agreement between the experimental data and the theoretical fitting curve. As a result, the sign of the amplitude of the very fast phases at both NaCl concentrations was positive, although the sign of the amplitude of the very fast phase observed by the chromophore fluorescence was negative.

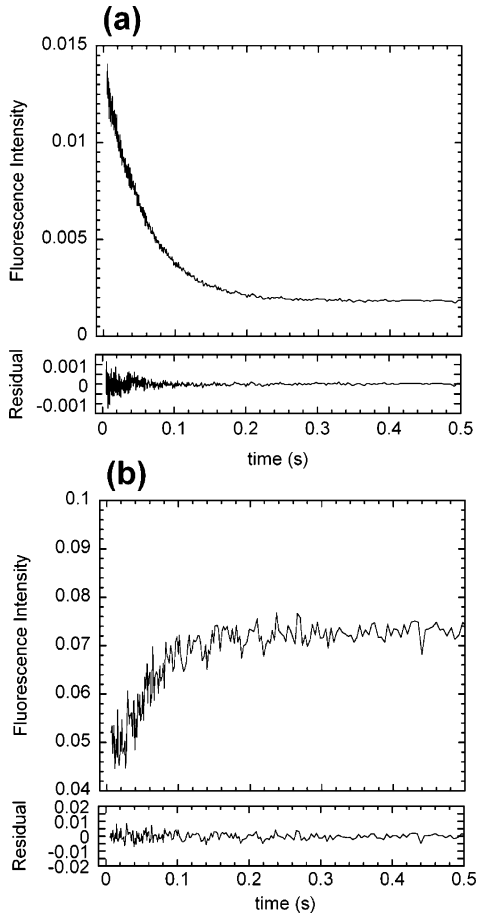

FIGURE 6: Kinetic unfolding curves monitored by the chromophore fluorescence excited at 395 nm (a) and the tryptophan fluorescence excited at 295 nm (b). The lower panel in each figure shows the residual plot. The reactions were initiated by a pH jump from pH 7.5 or 7.0 at 0 M NaCl to pH 2.0 at 0 M NaCl.

(2) Unfolding. Figure 6 shows typical kinetic unfolding curves measured by the chromophore fluorescence excited at 395 nm and the tryptophan fluorescence excited at 295 nm, respectively. The unfolding reactions were induced by pH jumps from the native state at pH 7.5 in a 10 mM Tris-HCl buffer solution to various pH values in the absence and presence of 0.10 M NaCl (see Figure 5a). All of the unfolding curves monitored by the chromophore fluorescence at 0.10 M (pH 2.0−4.1) and at 0 M NaCl (pH 2.5 and below) were fitted with a single exponential after a rapid decrease in fluorescence occurring within 5 ms. The apparent rate constant of unfolding was strongly dependent on pH and increased with decreases in pH (Figure 5a). The unfolding curves at 0 M NaCl had an additional faster phase at pH 3.0 and above. The unfolding rates monitored by tryptophan fluorescence and chromophore fluorescence at pH 2.0 and 0 M NaCl were essentially the same.

Interrupted Unfolding. To investigate whether the observed slow refolding phases were related to slow isomerization reactions in the denatured state (e.g., *cis/trans* isomerization of peptidyl−prolyl bonds), we carried out native to denatured to native (NDN) double-jump (interrupted unfolding) experiments in the stopped-flow apparatus; Cycle3 has 10 proline residues, and one of them has the *cis* configuration in the native structure. The protein in the native state was acid-denatured by the first pH jump from pH 7.5 to pH 2.0, and

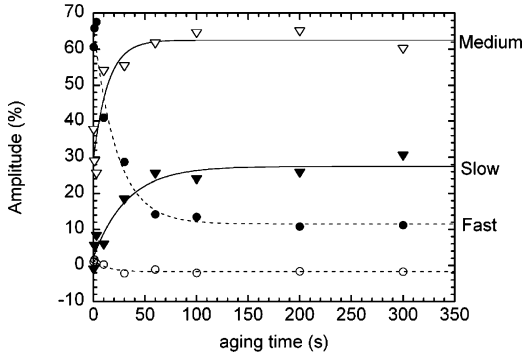

FIGURE 7: Normalized amplitudes of the refolding of Cycle3 as a function of the aging time measured by chromophore fluorescence excited at 395 nm. We fitted the data by fixing the rate constants of the very fast (open circles), fast (closed circles), medium (open triangles), and slow (closed triangles) phases to 4.60, 0.365, 0.0440, and 0.0144 s^{-1}, respectively, values which were obtained when we refolded the protein at 300 s after denaturing the protein.

it aged in the denatured state for a certain period of time (aging time, t_a). Then, the protein was refolded to the native state by the second pH jump from pH 2.0 to pH 7.5. When the protein was refolded immediately after being acid-denatured (i.e., $t_a \sim 0$), the refolding kinetics may not have included the slow phases. However, when the protein was refolded with a sufficiently long t_a, the refolding kinetics may have reflected the slow phases because the denatured protein with isomer states different from those of the native state accumulate while aging.

Figure 7 shows the relative amplitudes of the fast, medium, and slow phases of the refolding of Cycle3, as measured by the chromophore fluorescence and as a function of the aging time. The amplitude of the slow phase was zero at $t_a = 0$ and increased with increasing t_a. The t_a-dependent increase in the amplitude revealed single-exponential kinetics with a rate constant of 0.031 s^{-1}. The amplitude of the medium phase was 28% at $t_a = 0$, and it increased with t_a; this increase also revealed single-exponential kinetics with a rate constant of 0.071 s^{-1}. These rate constants of the t_a-dependent increase in the amplitudes of the slow and medium phases were found to be similar to known rate constants for the *cis*/*trans* isomerization of peptidyl−prolyl bonds (*23*). These results thus strongly suggest that the slow phase of the refolding of Cycle3 can be fully attributed to proline isomerization and, furthermore, that the medium phase of refolding can be partly attributed to isomerization in the denatured state.

Effect of Cyclophilin A on Folding Kinetics. To validate the contribution of proline *cis/trans* isomerization to the medium and slow phases of the folding kinetics, we measured the kinetic refolding of Cycle3 in the presence of CyPA, which has PPIase (peptidyl−prolyl isomerase) activity, i.e., the ability to accelerate the proline isomerization step (*23*). Figure 8 shows the refolding curves in the presence and absence of CyPA; the refolding was induced by manual mixing, such that we were unable to observe the very fast phase. The refolding of Cycle3 is apparently accelerated by CyPA. The refolding curve was fitted with three exponentials in the absence of CyPA and with two exponentials in the presence of CyPA (Table 3). As a result, the slow phase disappeared, the amplitude of the medium phase decreased, and the amplitude of fast phase increased in the presence of

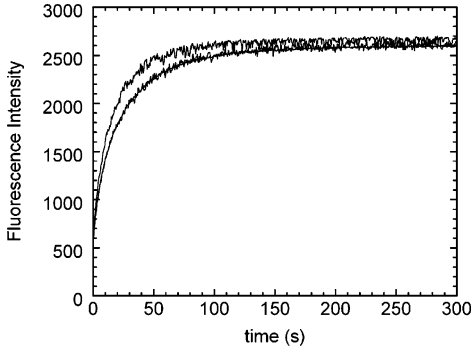

FIGURE 8: Kinetic refolding curves monitored by chromophore fluorescence in the presence and in the absence of CyPA. The upper and lower lines show the refolding curves in the presence and absence of CyPA, respectively.

Table 3: Rate Constants and Normalized Amplitudes of Refolding Curves of Cycle3 Measured by Chromophore Fluorescence in the Absence and Presence of CyPA

		rate constant k (s^{-1}) and normalized amplitude A (%)		
		fast[a]	medium	slow
−CyPA	k	0.153 ± 0.013	0.0312 ± 0.0011	0.00481 ± 0.00060
	A	47	49.9 ± 1.3	5.4 ± 0.5
+CyPA	k	0.111 ± 0.009	0.0323 ± 0.0014	
	A	61.8	38.2 ± 3.0	

[a] The amplitudes of the fast phase may represent the sum of the faster reactions.

CyPA. These results thus demonstrate the contribution of proline isomerization to the medium and slow phases of the folding kinetics of Cycle3.

DISCUSSION

The present study is the first in which the fast kinetics of GFP refolding from a denatured state have been characterized quantitatively by a variety of stopped-flow techniques. Previous studies on the folding of GFP include those by Fukuda et al. (*10*), Battistutta et al. (*11*), Iwai et al. (*12*), and Merkel and Regan (*13*). In all of these studies, the folding kinetics were monitored by chromophore fluorescence and were analyzed with a single exponential or with double exponentials, and the rapid reactions were ignored because the studies employed manual mixing to initiate the folding reactions. Recently, a pressure-jump study on the fast kinetics of GFP refolding from a high-pressure state (∼4 kbar) was reported by Herberhold et al. (*16*). However, the high-pressure state was only slightly unfolded and was not accompanied by any significant changes in the secondary structure of the backbone. Refolding from the high-pressure state was thus measured only by chromophore fluorescence. The rapid folding reactions of GFP from an extensively unfolded state (the acid-denatured state) monitored by stopped-flow CD, as well as by fluorescence techniques, are reported here for the first time.

In the present study, we investigated the folding and unfolding of GFP without observing any changes in the chemical structure of the *p*-hydroxybenzylideneimidazolidone chromophore, which remained intact in the denatured state. As a result, we were able to utilize the green fluorescence of the chromophore as a useful probe to monitor the formation of the native structure. However, it should be

mentioned in this context that the present results are in contrast with the in vivo GFP folding results starting with a translated polypeptide, in which the formation of most of the native backbone topology of GFP may be required before the chromophore is formed; moreover, chromophore formation itself has also been shown to be a very slow reaction (*4*).

At this point, it would be helpful to discuss in more detail the folding kinetics and folding intermediates of GFP, the rate-limiting step of GFP folding, and finally the mechanism of GFP folding on the basis of the results presented above.

Comparison of the Refolding Kinetics from the Acid-Induced and the Denaturant-Induced Denatured States. The present results regarding the refolding kinetics starting from the acid-denatured state of Cycle3 may be compared with the known refolding kinetics starting from the denaturant-induced denatured state. Fukuda et al. (*10*) and Battistutta et al. (*11*) have analyzed the refolding kinetics of Cycle3 from the fully unfolded state in concentrated GdnHCl and urea, respectively, by fluorescence spectroscopy, and they analyzed the dependence of the refolding rate constant on the denaturant concentration. Although their refolding curves are fitted with two exponentials, the rate constants extrapolated to 0 M denaturant (GdnHCl or urea) are in good agreement with the rate constants of the fast, medium, and slow phases observed in the present study. The fast phase reported in both studies is coincident with the fast phase in the present study, and the slow-phase rate constant reported in those studies lies between the medium and slow phases of the present study. Therefore, we concluded that the refolding kinetics of Cycle3 were independent of the initial denaturing conditions (i.e., the acid-denatured or denaturant-induced denatured), and instead these kinetics were thought to be solely determined by the refolding conditions, at least with respect to the reactions following the dead time occurring during manual mixing.

Folding Intermediates of Cycle3. There were at least two folding intermediates observed here, i.e., a burst-phase intermediate and an on-pathway intermediate, observed in the kinetic refolding of Cycle3 from the acid-denatured state.

(i) The Burst-Phase Intermediate. The burst-phase intermediate of refolding, which was formed within the dead time of the stopped-flow measurements, was characterized by a 621% change relative to the total change observed between the denatured and the refolded states in tryptophan fluorescence intensity (~350 nm) (Figure 4b), as well as by a change of the CD ellipticity at 225 nm, which was approximately 30% of the total change that was observed between the denatured state and the native state. However, the chromophore fluorescence detected by a high-pass filter above 460 nm was still zero in the burst-phase intermediate.

The above results strongly suggested that the burst-phase intermediate corresponds to a nonspecific collapsed ensemble of partially structured conformations of the protein. Because Trp57 is the only tryptophan residue of Cycle3, the increase in the tryptophan fluorescence suggested that the side chain of Trp57 is buried in a hydrophobic environment, sequestered from solvent water. The observed change in the far-UV ellipticity also suggested the formation of some secondary structure. However, the absence of chromophore fluorescence indicated that there is no rigid specific structure in the vicinity of the chromophore, and this variability of the structure would render the chromophore accessible to solvent water molecules that would then quench the chromophore fluorescence. The overall shape of the molecule might not be very compact, as was suggested by the substantial level of tryptophan fluorescence intensity. Although the fluorescence of Trp57 was effectively quenched by the chromophore in the native state, it was not quenched in the burst-phase intermediate, thus indicating that the distance between the tryptophan side chain and the chromophore is still sufficiently long enough to prevent the effective transfer of fluorescence energy from the tryptophan to the chromophore.

(ii) The On-Pathway Intermediate. The lag phase measured by the chromophore fluorescence that monitored the formation of the native state is a strong indication of the presence of the on-pathway folding intermediate. The accumulation of the intermediate resulted in a lag in the formation of the native state, leading to the negative amplitude measured by the chromophore fluorescence (Table 2). However, this lag phase corresponded to the very fast fluorescence- and CD-decreasing phases when it was measured by tryptophan fluorescence and the far-UV CD, respectively, indicating that the on-pathway intermediate is more nativelike than the burst-phase intermediate, at least when measured by these probes.

Both the burst-phase intermediate and the intermediate produced during the lag phase are thus assumed to be productive on-pathway intermediates. If the increase and subsequent rapid decrease in the tryptophan fluorescence in Figure 4b be a consequence of a non-native or an off-pathway state, the folding mechanism of GFP must become much more complicated; the tryptophan residue must first be buried to form the non-native structure, then the structure is disrupted, and finally the tryptophan is buried again to form the native structure, in which the tryptophan fluorescence is quenched by the chromophore. Although this might not be fully excluded, we do not further consider this possibility. According to the X-ray structure of GFP, Trp57 is located in the most hydrophobic region of the molecule and surrounded by Phe46, Cys48, Leu53, Leu60, Phe64, Tyr143, and Met218, while the *p*-hydroxybenzylideneimidazolidone chromophore is located in a hydrophilic region, forming hydrogen bonds with Glu94, Arg96, His148, Thr203, Glu222, and internal water molecules. It is thus likely that the nativelike hydrophobic contacts around the tryptophan residue form first in the burst phase intermediate, which is followed by formation of the more compact on-pathway intermediate.

From the above results, it appears likely that the on-pathway intermediate is a compact intermediate with a significant amount of secondary structure, but this intermediate was not found to have a specific rigid structure in the vicinity of the chromophore. Therefore, this intermediate reflects the typical characteristics of the molten globule state. The rapid decrease in tryptophan fluorescence was probably caused by the quenching of fluorescence emissions by the *p*-hydroxybenzylideneimidazolidone chromophore. The overall shape of the protein molecule is thus assumed to be sufficiently compact to allow the tryptophan fluorescence energy to be transferred by the chromophore. However, this intermediate still lacks specific rigid structure in the vicinity of the chromophore, such that the chromophore fluorescence is quenched by solvent water molecules.

The results of the present study also suggested that the structure of the intermediate of Cycle3 is highly heterogeneous; one side of the molecule (i.e., that including Trp57) is more rigid than the other side of the molecule that includes the chromophore. Trp57 is located at the end of the central helix and is in contact with the residues (Phe46, Cys48, Phe64, Tyr143, Leu53, Asp216, and Met218) of β-strand 3, β-strand 11, and a loop between strand 3 and the central helix. The large hydrophobic domain is formed by six β-strands (1−3, 5, 6, and 11), a loop, and central helices that connect β-strands 3 and 4. On the other hand, the *p*-hydroxybenzyl group of the chromophore faces toward β-strands 7 and 8 and forms a hydrogen bond with strands 4, 7, 8, 10, and 11 directly or through buried water molecules. In the crystal structure of GFP, the number of hydrogen bonds between β-strands 7 and 8 is smaller and the distance between these strands is longer than those between the other strands. Seifert et al. (*14*) have shown that one side of the protein, composed of β-strands 7−10, exhibits increased H−D exchange rates, and Helms et al. (*24*) have shown that the β-barrel of GFP is interrupted only between β-strands 7 and 8 according to a 1 ns molecular dynamics simulation. Therefore, it is very likely that this side (β-strands 7−10) of the protein is disrupted in the on-pathway folding intermediate, which renders the chromophore accessible to solvent water, whereas the other side (β-strands 3 and 11) of the molecule is more highly organized.

Rate-Limiting Step of GFP Folding (Slow Isomerization in the Denatured and the Intermediate States). The results of the NDN double-jump experiments have shown that the majority of the refolding kinetics of Cycle3 is rate-limited by slow isomerization in the denatured and the intermediate states (Figure 7). The slow phase that had a rate constant of $\sim$0.006 s^{-1} was fully rate-limited by the slow isomerization in the denatured and the intermediate states, because the amplitude was zero when the aging time in the NDN double-jump experiments was zero. However, the medium phase that had a rate constant of $\sim$0.03 s^{-1} was a composite of slow isomerization in the denatured and intermediate states and the real folding reaction, because the amplitude was not zero but instead was reduced to 29% of the total change of the chromophore fluorescence observed during the refolding when the aging time was zero.

The slow isomerization of Cycle3 in the denatured and intermediate states corresponded to the *cis*−*trans* isomerization about peptidyl−prolyl bonds. GFP has 10 proline residues, one of which is in the *cis* configuration in the native state (Figure 9). The rate constants of the slow and medium phases were both consistent with the known rate constants of the proline isomerization reactions of globular proteins. The results of CyPA experiments, in which the slow phase and a portion of the medium phase disappeared and accelerated in the presence of 2.1 μM CyPA, further validated the contributions of the prolyl isomerization to the slow phase and to some of the medium phase.

GFP Folding Mechanism. Scheme 1 represents a simplified scheme of the GFP (Cycle3) folding process, as deduced from the results of the present study. First, the denatured GFP, which involves at least two denatured species (D_F and D_S), forms the burst-phase intermediate (Ib_F and Ib_S) within the dead time of the stopped-flow measurements and then refolds to the on-pathway molten globule intermediate ($I1_F$, $I2_F$, $I1_S$, and $I2_S$) rapidly, i.e., in $\sim$0.5 s. The fast folding species (D_F) that has the same peptidyl−prolyl bond configurations as those of the native state refolds to $I1_F$ and $I2_F$ (0.5 s) through parallel pathways, and this species further refolds to the native state (N) in the fast (6−7 s) and medium phases (30−40 s). The slow-folding species (D_S) has nonnative peptidyl−prolyl bond configurations, and hence these species refold to the native state via the isomerization step in the molten globule intermediate state ($I1_F \leftrightarrow I1_S$ and $I2_F \leftrightarrow I2_S$) with the rate constant of the slow and medium phases.

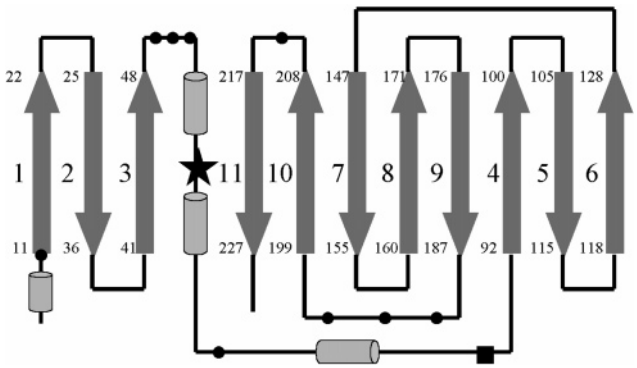

FIGURE 9: Schematic diagram of the secondary structure components of GFP (Cycle3). The black square and circles show the proline residues of the *cis* and *trans* conformations, respectively.

Scheme 1: A Simplified Scheme of GFP (Cycle3) Folding

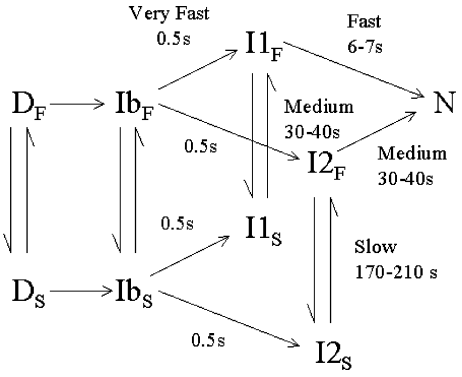

CONCLUSIONS

In the present study, we monitored the refolding of Cycle3 from the acid-denatured state by chromophore fluorescence, tryptophan fluorescence, and far-UV CD using stopped-flow apparatus. As a result, the refolding kinetics were found to involve five kinetic phases. These results, when taken together with the results of NDN (interpreted unfolding) double-jump experiments, suggested the following conclusions: (1) The burst phase corresponds to the nonspecific collapse of the GFP molecule, in which Trp57 is shielded from solvent water; (2) the very fast phase corresponds to the formation of an on-pathway folding intermediate that has the characteristics of the molten globule state; (3) the fast phase and some of the medium phase correspond to the direct refolding from the intermediate with the native proline configurations to the native state; and (4) the slow phase and a major portion of the medium phase are rate-limited by slow prolyl isomerization that takes place in the intermediate state, and this is a major portion of the observed kinetics involved in GFP folding.

REFERENCES

1. Ormo, M., Cubitt, A. B., Kallio, K., Gross, L. A., Tsien, R. Y., and Remington, S. J. (1996) Crystal structure of the *Aequorea victoria* green fluorescent protein, *Science 273*, 1392−1395.
2. Yang, F., Moss, L. G., and Phillips, G. M. (1996) The molecular structure of green fluorescent protein, *Nat. Biotechnol. 14*, 1246−1252.
3. Heim, R., Prasher, D. C., and Tsien, R. Y. (1994) Wavelength mutations and posttranslational autoxidation of green fluorescent protein, *Proc. Natl. Acad. Sci. U.S.A. 91*, 12501−12504.
4. Reid, B. G., and Flynn, G. C. (1997) Chromophore formation in green fluorescent protein, *Biochemistry 36*, 6786−6791.
5. Cubitt, A. B., Heim, R., Adams, S. R., Boyd, A. E., Gross, L. A., and Tsien, R. Y. (1995) Understanding, improving and using green fluorescent proteins, *Trends Biochem. Sci. 20*, 448−455.
6. Weissman, J. S., Rye, H. S., Fenton, W. A., Beechem, J. M., and Horwich, A. L. (1996) Characterization of the active intermediate of a GroEL-GroES-mediated protein folding reaction, *Cell 84*, 481−490.
7. Makino, Y., Amada, K., Taguchi, H., and Yoshida, M. (1997) Chaperonin-mediated folding of green fluorescent protein, *J. Biol. Chem. 272*, 12468−12474.
8. Martin, J. (2002) Requirement for GroEL/GroES-dependent protein folding under nonpermissive conditions of macromolecular crowding, *Biochemistry 41*, 5050−5055.
9. Ueno, T., Taguchi, H., Tadakuma, H., Yoshida, M., and Funatsu, T. (2004) GroEL mediates protein folding with a two successive timer mechanism, *Mol. Cell 14*, 423−434.
10. Fukuda, H., Arai, M., and Kuwajima, K. (2000) Folding of green fluorescent protein and the cycle3 mutant, *Biochemistry 39*, 12025−12032.
11. Battistutta, R., Negro, A., and Zanotti, G. (2000) Crystal structure and refolding properties of the mutant F99S/M153T/V163A of the green fluorescent protein, *Proteins 41*, 429−437.
12. Iwai, H., Lingel, A., and Plückthun, A. (2001) Cyclic green fluorescent protein produced in vivo using an artificially split PI-PfuI intein from *Pyrococcus furiosus*, *J. Biol. Chem. 276*, 16548−16554.
13. Merkel, J. S., and Regan, L. (2000) Modulating Protein Folding Rates *in Vivo* and *in Vitro* by Side-chain Interactions between the Parallel β Strands of Green Fluorescent Protein, *J. Biol. Chem. 275*, 29200−29206.
14. Seifert, M. H. J., Georgescu, J., Ksiazek, D., Smialowski, P., Rehm, T., Steipe, B., and Holak, T. A. (2003) Backbone dynamics of green fluorescent protein and the effect of histidine 148 substitution, *Biochemistry 42*, 2500−2512.
15. Haupts, U., Maiti, S., Schwille, P., and Webb, W. W. (1998) Dynamics of fluorescence fluctuations in green fluorescent protein observed by fluorescence correlation spectroscopy, *Proc. Natl. Acad. Sci. U.S.A. 95*, 13573−13578.
16. Herberhold, H., Marchal, S., Lange, R., Scheyhing, C. H., Vogel R. F., and Winter, R. (2003) Characterization of the pressure-induced intermediate and unfolded state of red-shifted green fluorescent protein—a static and kinetic FTIR, UV/VIS and fluorescence spectroscopy study, *J. Mol. Biol. 330*, 1153−1164.
17. Crameri, A., Whiteborn, E. A., Tate, E., and Stemmer, W. P. C. (1996) Improved green fluorescent protein by molecular evolution using DNA shuffling, *Nat. Biotechnol. 14*, 315−319.
18. Arai, M., and Kuwajima, K. (2000) Role of the molten globule state in protein folding, *Adv. Protein Chem. 53*, 209−282.
19. Greenfield, N., and Fasman, G. D. (1969) Computed circular dichroism spectra for the evaluation of protein conformation, *Biochemistry 8*, 4108−4116.
20. Brahms, S., and Brahms, J. (1980) Determination of protein secondary structure in solution by vacuum ultraviolet circular dichroism, *J. Mol. Biol. 138*, 149−178.
21. Bokman, S. H., and Ward, W. W. (1981) Renaturation of *Aequorea* green-fluorescent protein, *Biochem. Biophys. Res. Communn. 101*, 1372−1380.
22. Ward, W. W., and Bokman, S. H. (1982) Reversible denaturation of *Aequorea* green-fluorescent protein: physical separation and characterization of the renatured protein, *Biochemistry 21*, 4535−4540.
23. Balbach, J., and Schmid, F. X. (2000) *Mechanism of Protein Folding* (Pain, R. H., Ed.) 2nd ed., pp 212−249, Oxford University Press, Oxford, U.K.
24. Helms, V., Straatsma, T. P., and McCammon J. A. (1999) Internal dynamics of green fluorescent protein, *J. Phys. Chem. B 103*, 3263−3269.

BI048733+